Human health risk assessment and spatial distribution of fluoride from shallow groundwater in a region of southwest China

Kai Zhang, Xiaonan Li, Xinhui Zheng, Changdi Qiang and Xinghao Zhang

ABSTRACT

This article took fluoride in shallow groundwater of a township in southwestern China as the research object. Fifty sampling points were set up in the studied area. The fluoride was tested by the ion-selective electrode method. The health risk model recommended by the United States Environmental Protection Agency was used. Based on the Chinese population, human health risk assessment was performed for fluoride in shallow groundwater in the studied area, and the Kriging interpolation method was used to simulate the spatial distribution of fluoride concentration in the area. The research showed the following. (1) The concentration of fluoride in the shallow groundwater samples in the studied area was 0.06–0.78 mg/L, with an average value of 0.35 mg/L, which was in line with the limit value (1.00 mg/L) in the standards for drinking water quality (GB 5749–2006), but its maximum value was 0.78 mg/L, which was 1.86 times of the background value. (2) The average hazard index of children and adults were 0.27 and 0.15, respectively, which were less than 1, and the risk was at an acceptable level; the noncarcinogenic risk of children was 1.8 times that of adults; the average values of total risk quotient for groundwater fluoride intake by children and adults were 0.27 and 0.15, respectively, and 1.19E-03 and 7.26E-04 by skin, respectively. This indicated that of the two routes, oral intake was the main route of exposure to fluoride. The noncarcinogenic risk values of fluoride in rural and urban areas were similar, and both were less than 1. (3) The high-value areas of fluoride were mainly concentrated in the southeast of the area, which was mainly affected by the superposition of natural factors and industrial park sewage discharge. Through human health risk assessment and spatial distribution of fluoride in regional groundwater, it can provide a theoretical basis for regional groundwater pollution prevention.

Key words | fluoride, human health risk assessment, shallow groundwater, spatial distribution

Kai Zhang (corresponding author)
Xiaonan Li
Xinhui Zheng
Changdi Qiang
Xinghao Zhang
School of Chemistry and Environment,
China University of Mining and Technology (Beijing),
Ding 11, Xueyuan Road, Haidian District, Beijing, China
E-mail: *zhangkai@cumtb.edu.cn*

HIGHLIGHTS

- The human health risk assessment model was optimized concerning China's population parameters.
- Health exposure via multiple routes was assessed using the HHRA model.
- Employed Kriging model to identify fluoride spatial distribution.
- The impact of water quality on human health should be conducted with vigorous propaganda to heighten public awareness.

INTRODUCTION

Groundwater is the natural resource on which human beings depend for survival all over the world (Wu *et al.* 2012). With the rapid development of industry and the impact of human activities, groundwater pollution has become increasingly serious (Li *et al.* 2012). About 80% of diseases in the world are caused by poor water quality, of

doi: 10.2166/aqua.2020.060

which 65% are caused by endemic fluorosis (Felsenfeld & Roberts 1991; WHO 2011; Miri *et al.* 2016; Adimalla & Venkatayogi 2017; Karami *et al.* 2017; Narsimha & Sudarshan 2017). Fluoride is a nonmetallic chemical element, and it is also one of the essential trace elements in the human body. It has two sides (Zhang 2010). Long-term intake of drinking water with a low fluoride concentration (<0.50 mg/L) can lead to mild to moderate tooth decay in children, while high fluoride concentration (>1.50 mg/L) can lead to fluorosis (e.g. skeletal fluorosis) (Biglari *et al.* 2016), destroying blood cells, mucous membranes and intestines (Ozsvath 2009). Therefore, it is necessary to evaluate the human health risk and clarify the spatial distribution of risks for groundwater fluoride in the studied area.

In recent years, research into human health risk assessment of fluoride and its spatial distribution has been increasing. Human health risk assessment models are used to assess the adverse health effects on humans in the present and the future through exposure to chemicals and environmental factors (Patterson *et al.* 2002). Ganyaglo *et al.* (2019) conducted a human health risk study on groundwater fluoride in eastern Ghana, and the results indicated that all age groups in the studied area may face noncarcinogenic health risks. Hanse *et al.* (2019) used a human health risk model recommended by the United States Environmental Protection Agency (USEPA) to conduct a risk assessment of fluoride in groundwater in 8 blocks of Karbi Anglong. The results showed that the hazard quotient (HQ) ranges for adults and children were 0.06–10.70 and 0.20–35.00, respectively. Zhang *et al.* (2017) evaluated the health risks of fluoride exposure to Chinese residents in improved drinking water. The results showed that 95% of children's noncarcinogenic risks exceeded safe level 1. The aforementioned studies all used the USEPA health risk assessment model for the risk assessment of fluoride. It can be seen that this model was widely accepted in risk assessment, so this article chose it as the evaluation model. However, most of the model parameters were not modified according to the national environment. In the application process, the model parameters should be adjusted according to the actual human exposure characteristics to evaluate the human health risk caused by groundwater fluoride in the studied area.

The combination of geostatistics and geographic information system (GIS) technology can be used to identify the spatial relationship between environmental parameters and the impact of human health (Abbasnia *et al.* 2019) and to visualize its spatial distribution. Aghapour *et al.* (2018) used GIS to analyze the experimental results, which showed that the levels of F in groundwater in the western and southern parts of the study area were less than 0.50 mg/L, which was the recommended value for controlling dental caries (0.50–1.00 mg/L). Fallahzadeh *et al.* (2018) used GIS to investigate the distribution of F^- in drinking water in Yazd Province, Iran, and the results showed that Ashkeesal had the highest F^- concentration and more attention should be paid to the health of residents. Li *et al.* (2019) used GIS software to explore the distribution of F^- in drinking water in the studied area. The results showed that high F^- concentration was found in GJ and QX, and the drinking water with high F^- concentration came from wells in suburbs or mining areas. Xu & Zhang (2018) used GIS spatial analysis tools to visually display and statistically analyze the spatial distribution characteristics of risks of different exposed populations.

This study collected the shallow groundwater of a township in southwestern China as the research object and used the local groundwater background value to evaluate the fluoride pollution situation. The USEPA human exposure risk model was selected, and the model parameters were referenced to the Chinese population parameters in the Technical Guidelines for Risk Assessment of Contaminated Sites issued by the Ministry of Environmental Protection in 2014 (HJ25.3-2014) (Ministry of Environmental Protection of the PRC 2014). The parameters were revised to evaluate the noncarcinogenic risk of fluoride to children and adults in the region and its noncarcinogenic risk to different functional areas. The Kriging interpolation method was introduced to simulate the spatial distribution of fluoride in the studied area to fit the continuous distribution map of fluoride concentration in the studied area, to accurately predict the pollution situation, which was helpful to assess the human health risk and spatial distribution characteristics of fluoride in detail and accurately, and to provide a theoretical basis for the monitoring and prevention of fluoride in shallow groundwater in this area.

MATERIALS AND METHODS

Study area

The study area is located in the northeast of the central part of Guangxi Province, and its geographical coordinates are between 24°25′32.69″–24°29′22.17″ north latitude and 109°39′00.59″–109°47′35.11″ east longitude. It belongs to the transition zone from the south subtropical to the middle subtropical zone, with the mild climate and abundant rainfall, but uneven distribution, the drought and flood are obvious. During the rainy season, rainwater will bring a lot of soluble substances from the soil surface to the soil environment and eventually into groundwater through leaching. There is a Longsheng-Yongfu fault zone in the studied area, and no obvious adverse geological effect is seen on the site. Because the area is surrounded by mountain forests, groundwater in mountain forest areas is not easy to collect and is rarely used directly by humans. Therefore, this study only selected regional groundwater with human activities for research. The groundwater in the area is mainly replenished by atmospheric precipitation and irrigation water infiltration. It consists of a fissure hole (karst) water and bedrock fissures. It is only used for fetching water from scattered small wells, mainly for domestic water and a small amount for irrigation. There is no industrial mining value. There is an underground watershed in the area from the southwest to the northeast. The watershed and the mountain regions of the northwest and southeast have the highest groundwater potential energy, while the two main rivers are the lowest potential energy locations. The groundwater in the studied area is composed of two mountainous areas and watersheds flowing into two surface rivers. According to survey statistics, the existing factories in the studied area are mainly located in the southeast part of the middle, with a total of 14 factories. Among them, there is a large industrial park in the middle, and several industrial factories are concentrated in the industrial park. Besides this, there is a large-scale food factory and paper mill outside the industrial park, which are located on the west side of the industrial park and the southwest side of the research area. The schematic diagram of the location of the research area is shown in Figure 1.

Sample collection

Based on local actual conditions and meeting Kriging interpolation simulation requirements, a total of 50 groundwater

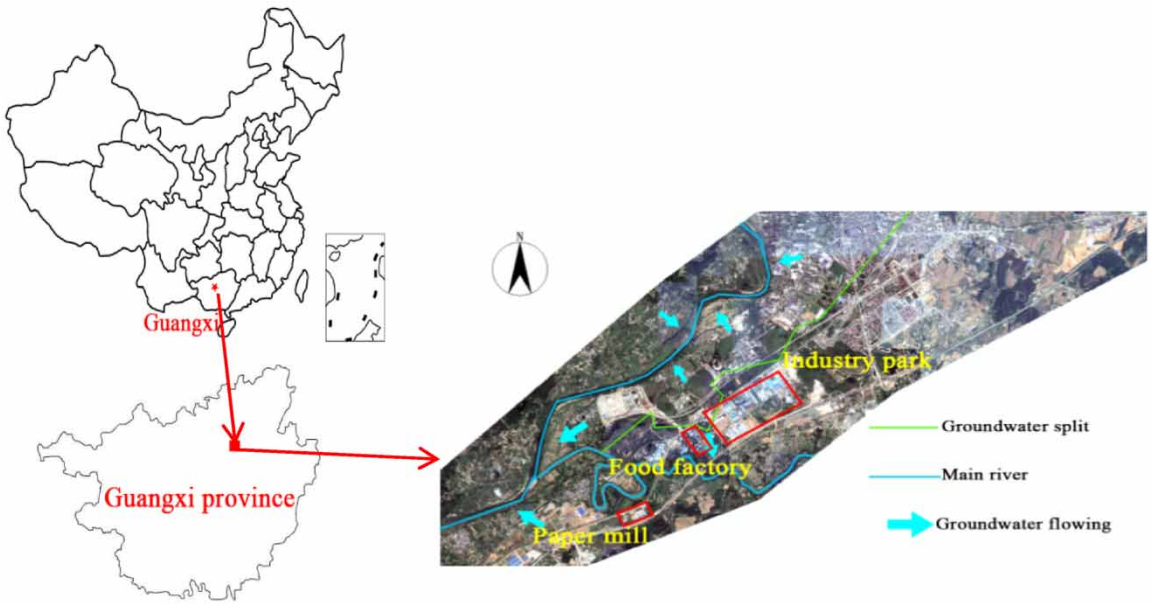

Figure 1 | Schematics of the study site.

samples were collected in this study, including 20 monitoring well water samples, 19 self-jetting water samples, and 11 nonjetting water samples. The northwest of the area is a mountain forest area. The groundwater in the mountain forest area is not easy to collect and is rarely used directly by people. The two mountainous regions in the northwest and southeast are the locations with higher groundwater potential energy, while the two major rivers are the lowest. The pollutants in the areas with the higher potential energy of underground water will migrate with the underground water flow field, which may eventually gather and accumulate in the two river areas. Therefore, three sampling points (self-jetting wells) were selected in a relatively clean area in the northwest. The average value of the water quality index was taken as the background value of the groundwater environmental quality in the studied area. The distribution of sampling points and background points are shown in Figure 2.

According to the Groundwater Environmental Monitoring Technical Specification (HJ-T 164-2004) (Ministry of Environmental Protection of the PRC 2004): (1) when the sampling point is a groundwater monitoring well, the groundwater level is measured by the groundwater level gauge first, the water is pumped from the well, and the groundwater collector is put into the well to collect a small amount of water for the fluoride test and analysis. After that, the water sample is poured out for testing, sufficient water sample is taken again and sealed in a plastic bucket (1.00 L) and brought to the laboratory for testing. (2) When the sampling point is self-sprayed spring water, the water sample is directly collected at the center of the spring mouth, discarded after testing for fluoride, after which a sufficient amount of water sample in a plastic bucket is recollected and sealed for testing. (3) When the sampling point is spring water that is not self-spraying, the remaining water is pumped away first and then the new water is replaced, and the field test and sampling are performed. The collected groundwater samples were labeled and sealed and sent to the laboratory within 24 hours for analysis at 4 °C. All precautions should be taken during sampling, handling, transportation, storage and analysis to avoid contamination of samples according to the American Public Health Association (APHA 2005).

Sample testing

The fluoride ion-selective electrode was used to electrochemically determine the fluoride concentration in groundwater

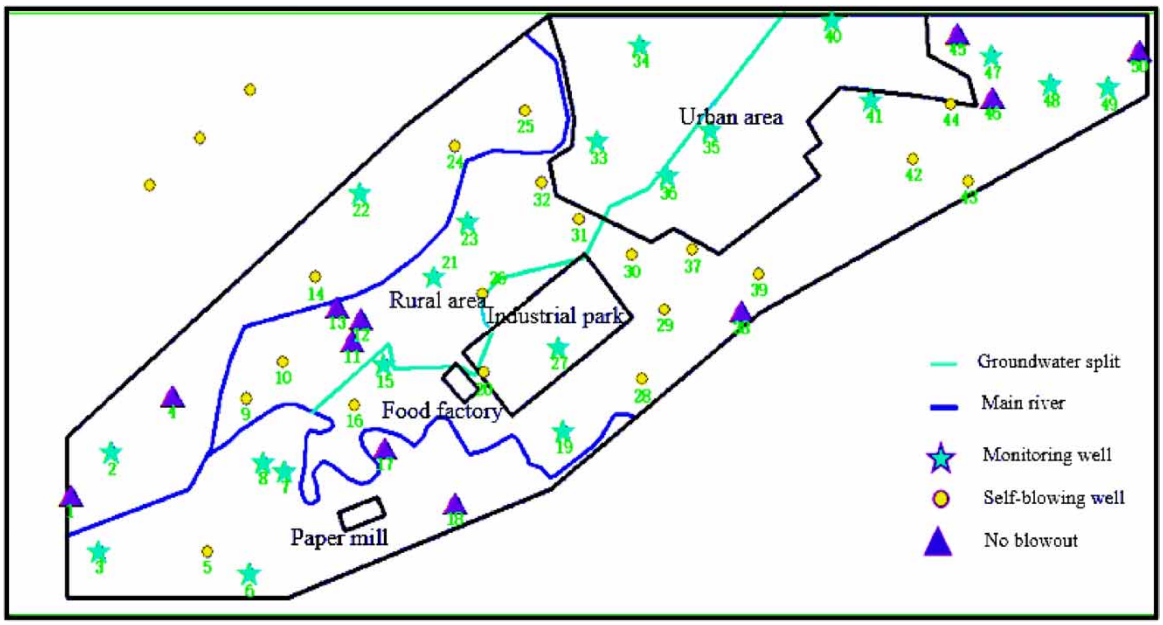

Figure 2 | Sampling point distribution map.

samples, and the detection limit was 0.02 mg/L. Sodium fluoride was a stock solution (100 ± 0.50 mg/L) and was serially diluted with distilled water to prepare a series of standard fluoride solutions (0.10–10.00 mg/L). The total ion strength adjusting buffer grade III (TISAB III) was added to all standards and samples at a ratio of 10: 1 to adjust the ionic strength and reduce interference from other ions. Before measuring the fluoride concentration, 20 ml of groundwater was extracted and 2 ml of TISAB was added. Analysis of the blanks, spiked and duplicate samples were carried out to check accuracy and precision (reproducibility) value of the instrument. The error of the results was ±2%. The samples were analyzed in triplicate, and the averages were recorded (Mukherjee *et al.* 2019).

Quality control

The reagents and re-distilled water used for solution preparation (or dilution) were analytical pure water (Merck Millipore) and microporous water with the highest purity, respectively. Quality assurance was achieved by implementing the standard laboratory procedures and quality control techniques described in APHA (APHA 2005).

Health risk assessment

According to the health risk assessment model recommended by the USEPA and the actual situation of human health in China and referring to USEPA (1989) and Wu & Sun (2016), the human health risk assessment of the shallow groundwater fluoride in the studied area was conducted. Two exposure routes, oral intake and skin contact, were selected to evaluate adults and children, respectively.

The calculation of the noncarcinogenic risk of oral intake is shown in formulas (1) and (2):

$$\mathrm{Intake}_{\mathrm{oral}} = \frac{C \times IR \times EF \times EW}{\mathrm{BW} \times \mathrm{AT}} \tag{1}$$

$$\mathrm{HQ}_{\mathrm{oral}} = \frac{\mathrm{Intake}_{\mathrm{oral}}}{\mathrm{RfD}_{\mathrm{oral}}} \tag{2}$$

Among them, $\mathrm{Intake}_{\mathrm{oral}}$ represents the average daily exposure dose (mg/kg/d) per unit weight by the oral route, and C is the concentration of the pollutant in water (mg/L). IR indicates the rate of water intake through drinking water (L/d). The water intake rate for adults is 1.50 L and for children under 12 years it is 0.70 L. EF and ED are the exposure frequency (d/a) and exposure duration (a), respectively. The EF of adults and children is 365 days a year, the ED of adults is 30 years and that of children is 12 years. The average BW for adults and children is 60 and 15 kg, respectively. AT is the average time for noncarcinogenic effects (d). The average time of adults and children is 10,950 days and 4,380 days, respectively. $\mathrm{HQ}_{\mathrm{oral}}$ represents the risk quotient of noncarcinogenic risks through the oral intake route, and $\mathrm{RfD}_{\mathrm{oral}}$ represents the reference dose of noncarcinogenic pollutants through the oral intake route, with a value of 0.06 (mg/kg/d) (IRIS 2016).

The noncarcinogenic risk calculation for the skin intake is shown in formula (3):

$$\mathrm{Intake}_{\mathrm{derm}} = \frac{\mathrm{DA} \times \mathrm{EV} \times \mathrm{SA} \times \mathrm{EF} \times \mathrm{ED}}{\mathrm{BW} \times \mathrm{AT}} \tag{3}$$

$$\mathrm{DA} = K \times C \times t \times CF \tag{4}$$

$$\mathrm{SA} = 238 \times H^{0.416} \times \mathrm{BW}^{0.517} \tag{5}$$

$$\mathrm{HQ}_{\mathrm{derm}} = \frac{\mathrm{Intake}_{\mathrm{derm}}}{\mathrm{RfD}_{\mathrm{derm}}} \tag{6}$$

$\mathrm{Intake}_{\mathrm{derm}}$ represents the average daily exposure dose (mg/kg/d) ingested through the skin per unit weight, EV is the daily exposure frequency of skin contact events (1/d) and the EV allocation for adults and children is 1. DA represents the exposure dose ($\mathrm{mg/cm^2}$) for each event and can be estimated using the equation as shown in formula (4). K is the skin's permeability coefficient (cm/h), C is the concentration of pollutants in water (mg/L) and t is the contact time of a shower (h/d). According to the statistical surveys, adults and children need about 0.4 h per day (Wu & Sun 2016). CF is a conversion factor equal to 1.00×10^{-3}. SA stands for the skin surface area and can be estimated using an empirical formula, as shown in formula (5). H represents a person's height, and the BW parameter value is consistent with the foregoing. $\mathrm{RfD}_{\mathrm{derm}}$

represents the reference dose of noncarcinogenic pollutants through the dermal route, with a derived value of 5.82×10^{-2} (mg/kg/d) (Staff 2001).

The calculation of the total noncarcinogenic risk is shown in formula (7):

$$HI = HQ_{oral} + HQ_{derm} \quad (7)$$

The total noncarcinogenic risk is represented by the hazard index (HI). $HI < 1$ indicates that the noncarcinogenic risk is acceptable, while $HI > 1$ indicates that the risk has exceeded an acceptable level.

Kriging interpolation

Kriging interpolation, also known as spatial local interpolation, is a linear, unbiased and optimal estimation method for unknown sampling points of regionalized variables based on spatial autocorrelation using the raw data of the regionalized variables and the structure of the semivariance function (Huang *et al.* 2010; Liu *et al.* 2010; Shi *et al.* 2017). Its formula is expressed as (Wang *et al.* 2008) follows:

$$Z_{(x_0)} = \sum_{i-1}^{n} \lambda_i Z_{(x_i)} \quad (8)$$

where $Z_{(x0)}$ is the sample content of the point to be estimated, n is the number of sampling points, $Z_{(xi)}$ is the content of the ith sampling point and λ_i is a set of weight coefficients that are estimated unbiased and have the smallest estimated variance.

The Kriging interpolation method should be based on the spatial autocorrelation test and a suitable interpolation method fitted by the variogram model (Li *et al.* 2013).

Software platform

All the sampling data were analyzed using SPSS 19.0.0 statistical software (SPSS, Chicago, USA). Spatial autocorrelation analysis, editing geographic information, spatial interpolation simulation and cross-checking were analyzed using ArcGIS 10.0 (Gamma Design Software, Plainwell, USA).

CONCLUSION AND DISCUSSION

Distribution characteristics of groundwater fluoride

The results of the character analysis of basic data of fluoride using SPSS are presented in Table 1. It can be seen from Table 1 that the fluoride in the groundwater samples in the studied area was 0.06–0.78 mg/L, with an average value of 0.35 mg/L, which was in line with the National Standards for Drinking Water Quality (GB5749-2006) (Ministry of Health of the PRC 2006) (≤1.00 mg/L). In the areas with the fluoride concentration lower than 0.50 mg/L, attention should be given to preventing the prevalence of dental caries in residents. However, the maximum fluoride was 0.78 mg/L, which reached 1.86 times the background value, and 34% of points exceeded the background value, indicating that its pollution trend was more obvious; the dispersion coefficient was 0.54, which belonged to medium variation, indicating that the accumulation of fluoride was obvious. Besides, it can be seen from the normality test that the K-S test *P*-value of the fluoride was greater than 0.05, which obeyed the normal distribution.

Health risk assessment of fluoride

The detection results of various samples of groundwater were brought into the model formula for calculation, and the results are shown in Figures 3 and 5.

Table 1 | Basic data characteristic analysis table

Water quality factor	Concentration range (mg/L)	Mean	Dispersion coefficient	Background value (mg/L)	Out-of-standard rate (based on background value)	K-S normal test *P*-value
Fluoride	0.06–0.78	0.35	0.54	0.42	34%	0.37

This study evaluated the noncarcinogenic health risks of oral intake (drinking) and skin intake (showering) fluoride to a township population in southwestern China. The results are shown in Figure 3. The average HI values of children and adults in the studied area were 0.27 and 0.15, respectively, which were less than 1, indicating that the shallow groundwater fluoride in the studied area was generally acceptable for noncarcinogenic risk to the human body. The highest values of HI in children and adults were 0.61 and 0.33, respectively. Based on the background concentration of fluoride, the HI values of children and adults were 0.33 and 0.18, respectively, indicating that the overall noncarcinogenic risk to children and adults was relatively high. Care should be taken to prevent the accumulation of fluoride from leading to high overall risk.

Children were found to have a higher noncarcinogenic risk of fluoride compared to adults. Descriptive statistics of HQ and HI values for the intake and skin contact pathways

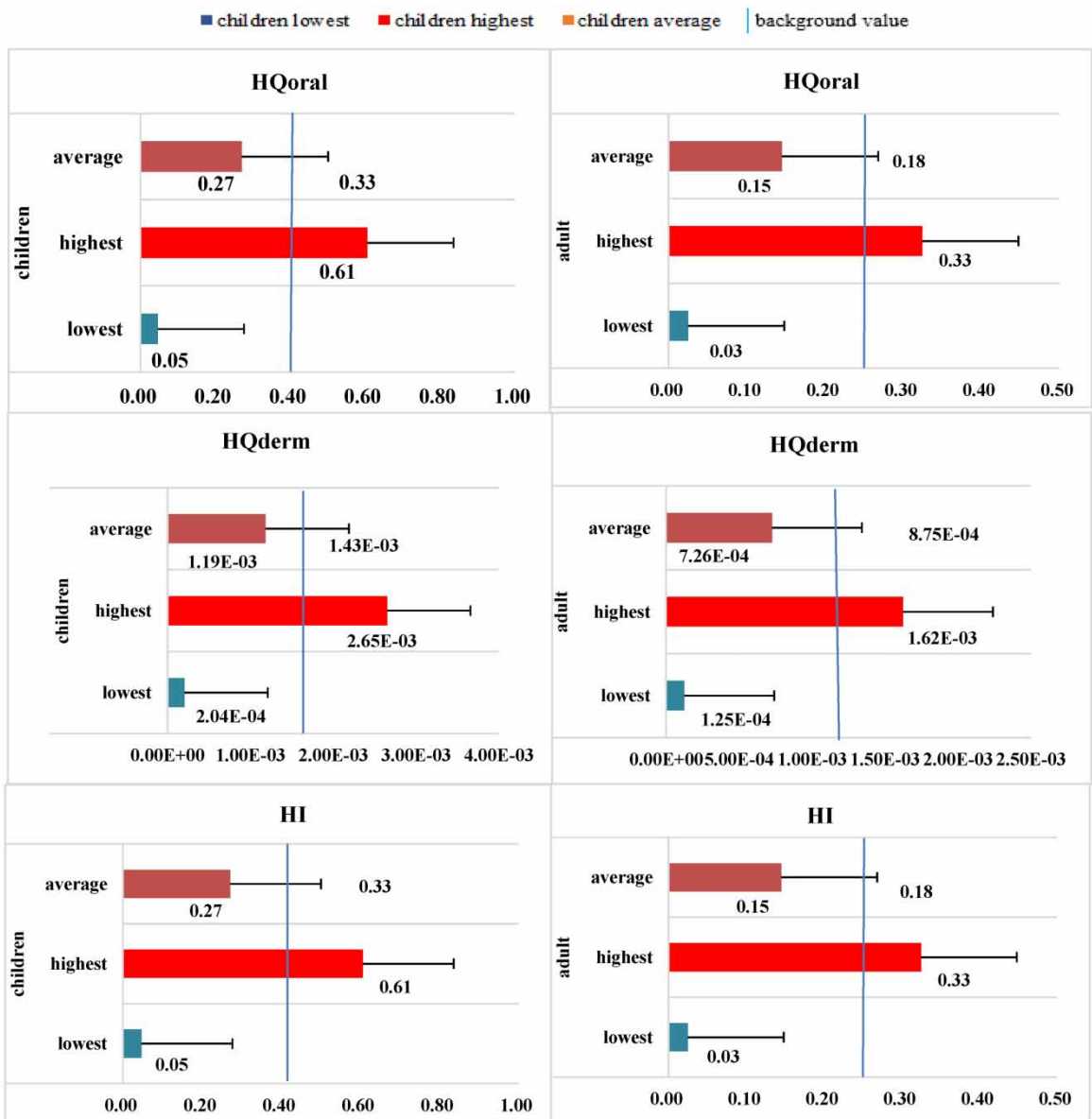

Figure 3 | Health risks of groundwater fluoride at different ages.

of children and adults are shown in Figure 3. In the studied area, children's noncarcinogenic risk quotients for groundwater fluoride intake orally and through skin were greater than adults, so the total noncarcinogenic risk index caused by fluoride was also greater than adults, 1.80 times that of the adults. It can be concluded that children are at the highest risk, followed by adults. Children are a vulnerable group. Compared to adults, children have a higher intake of fluoride, resulting in higher potential risks than adults. Research by Ahada & Suthar (2019) found that children were smaller than adults, and they accumulated more pollutants, making them more at risk for fluoride intake. The research conducted by Zhang *et al.* (2017) found that children's high risk was due to low body weight, which led to higher exposure doses, which was consistent with our findings. Besides, children are in an important period of growth and development, their metabolism is stronger than that of adults and their sensitivity to fluoride is higher than that of adults. Because fluoride is sensitive to developmental stages (in particular, the prenatal and postnatal adult stages, the first year of life and adolescence), children living in areas with the increased fluoride content often experience normal physical maturity and bone formation problems (Vyeltishchyev 1995). Zhang *et al.* (2019) conducted a health risk assessment of groundwater in a buckwheat field in Yunnan. The results showed that children's noncarcinogenic risk was 1.30 times that of adults, and their sensitivity to groundwater pollution factors was higher than that of adults. These support our findings that children are more sensitive to fluoride than adults. The occurrence of noncarcinogenic high-risk conditions for children with groundwater fluoride should be prevented.

Besides, the average risk quotient of noncarcinogenic risk of oral intake of groundwater fluoride in children and adults was 0.27 and 0.15, respectively, and the average risk quotient of noncarcinogenic risk of skin intake was 1.19E-03 and 7.26E-04, respectively, indicating that the noncarcinogenic risk of oral intake of groundwater fluoride in the studied area was higher than that of the skin route. Therefore, oral intake of drinking water was the main route of exposure to fluoride (WHO 2004). The pollutants in groundwater mainly enter the human body through two ways: direct drinking and skin contact. These two ways bring more than 90% pollutants in the human body (Wang *et al.* 2009). Among them, direct drinking is the main way for the human body to absorb pollutants in water. Compared with this, the impact of other ways can be ignored. Kumar *et al.* (2019) found that the average daily potential dose of fluoride ingested by drinking groundwater was higher than that absorbed by the skin in comparison with the risk assessment of the groundwater quality in Khar Pradesh. Zhang *et al.* (2017) found that the daily intake of fluoride in drinking water was three orders of magnitude higher than that absorbed by skin, and the noncarcinogenic risk of fluoride absorption through the skin was negligible, and the intake was the main route of exposure.

There are two functional areas in the studied area: urban and rural. As shown in Figure 4, the average concentrations of fluoride in shallow groundwater in urban and rural areas were 0.27 mg/L and 0.36 mg/L, respectively. The average

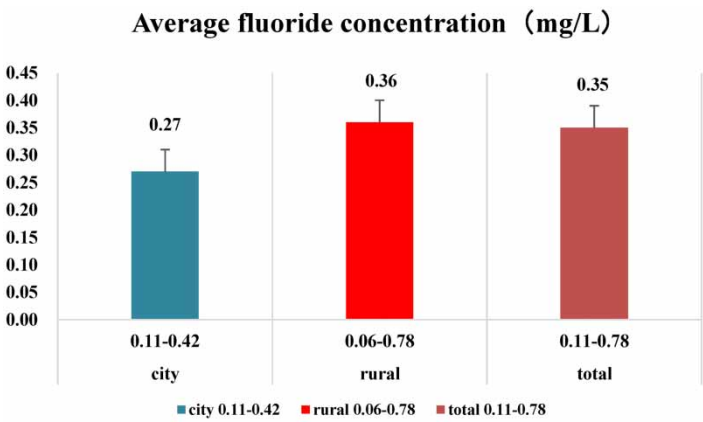

Figure 4 | Average fluoride concentration in different functional regions.

concentration was 0.35 mg/L. The results showed that the average concentration of fluoride in shallow groundwater in urban areas was lower than that in rural areas, and the high concentration values were mostly concentrated in rural areas. This result may be related to wastewater discharged by industrial parks, food factories and paper mills in rural areas. Besides, as shown in Figure 5, the HQ and HI of children in urban and rural areas was higher than that of adults, indicating that children were at high risk, and the HI values in both functional areas were less than 1, indicating that the noncarcinogenic risk of fluoride in shallow groundwater in urban and rural areas was acceptable.

Variogram model fitting

Spatial autocorrelation analysis

The spatial autocorrelation analysis of fluoride was performed using the spatial autocorrelation (Moran's I) tool in the ArcGIS spatial statistics tool.

Moran's index (Moran's I) is one of the commonly used methods to calculate spatial autocorrelation. When Moran's $I > 0$, the observation data have a positive spatial correlation. When Moran's $I < 0$, the observation data have a negative spatial correlation. When Moran's $I = 0$, the observation data are random (Cai *et al.* 2012). When calculating the Moran index, it is also necessary to judge the significance of the spatial autocorrelation according to the Z-value and the P-value. The basis for determining the spatial autocorrelation: when $|Z| \geq 2.58$, $P \leq 0.01$, it is very significant; when $|Z| \geq 1.96$, $P \leq 0.05$, it is significant; when $|Z| < 1.96$, $P > 0.05$, it is not significant (Fan *et al.* 2013).

As can be seen from Table 2, the Moran's I value of the fluoride was close to 1, so it showed a significant cluster and had a positive correlation. The spatial autocorrelation of these data was very significant, so the Kriging interpolation can be used to predict their spatial distribution.

Analysis of spatial variation structure

The theoretical models of variograms mainly include circle, spherical, Gaussian and exponential models (Zhong *et al.* 2009). The selection of the semivariance function model of fluoride is presented in Table 3.

According to Table 3, the C_0/sill of the four models for the simulation of fluoride spatial distribution was less than 75%, which meant that the change of fluoride content in groundwater in this area was more affected by regional factors than nonregional factors. The mean value and root mean square of the prediction error of the four models were not much different, and the mean value of the prediction error of the Gaussian model was the closest to 0, but the mean square root of the prediction error of the exponential model was closer to 1, so it was difficult to directly

Table 2 | Spatial autocorrelation test results

Test data	Moran's *I*	*Z*-value	*P*-value
Fluoride	0.66	6.42	0.00

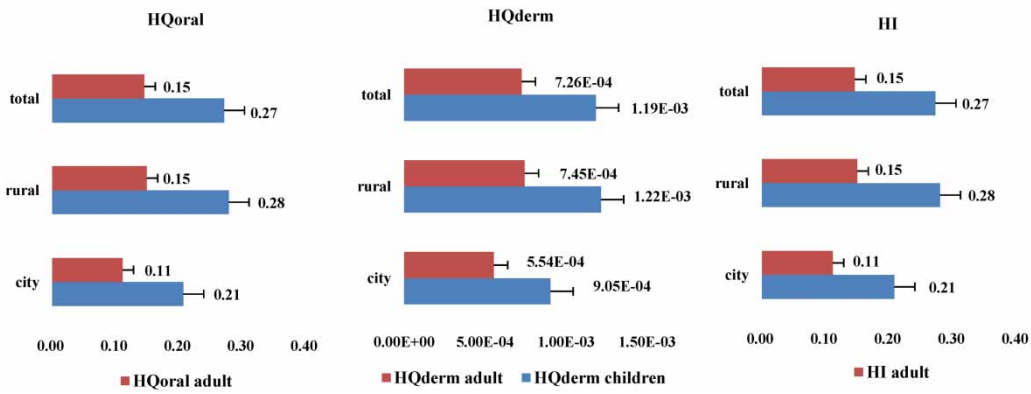

Figure 5 | Health risks of groundwater fluoride in different functional areas.

Table 3 | Analysis table of spatial variation structure of fluoride

Model	Nugget constant C_0	Sill	C_0/sill (%)	Error mean	Root-mean-square error
circle	2.00E-03	4.00E-03	5.43E-01	−2.10E-02	1.02E + 00
spherical	2.00E-03	4.00E-03	5.29E-01	−2.30E-02	1.02E + 00
Gaussian	2.00E-03	3.00E-03	6.29E-01	−1.70E-02	1.03E + 00
exponential	1.00E-03	4.00E-03	2.42E-01	−4.00E-02	9.86E-01

determine the best model. However, the prediction error of each model was close to 0, and the root mean square was also close to 1. It can be considered that the spatial distribution prediction of fluoride distribution in groundwater by four models was close to the real situation. Further screening can be carried out by cross-test results.

Figure 6 shows that there was no significant difference between the predicted value and the measured value under the four models, and the determined coefficients of the four models were all above 0.9, which was closer to 1 compared with the exponential model.

In summary, the exponential model was similar to the other four models in the mean and the root mean square of prediction error, the simulation effect on the close distance point was better, and the coefficient of determination was higher. Therefore, the exponential

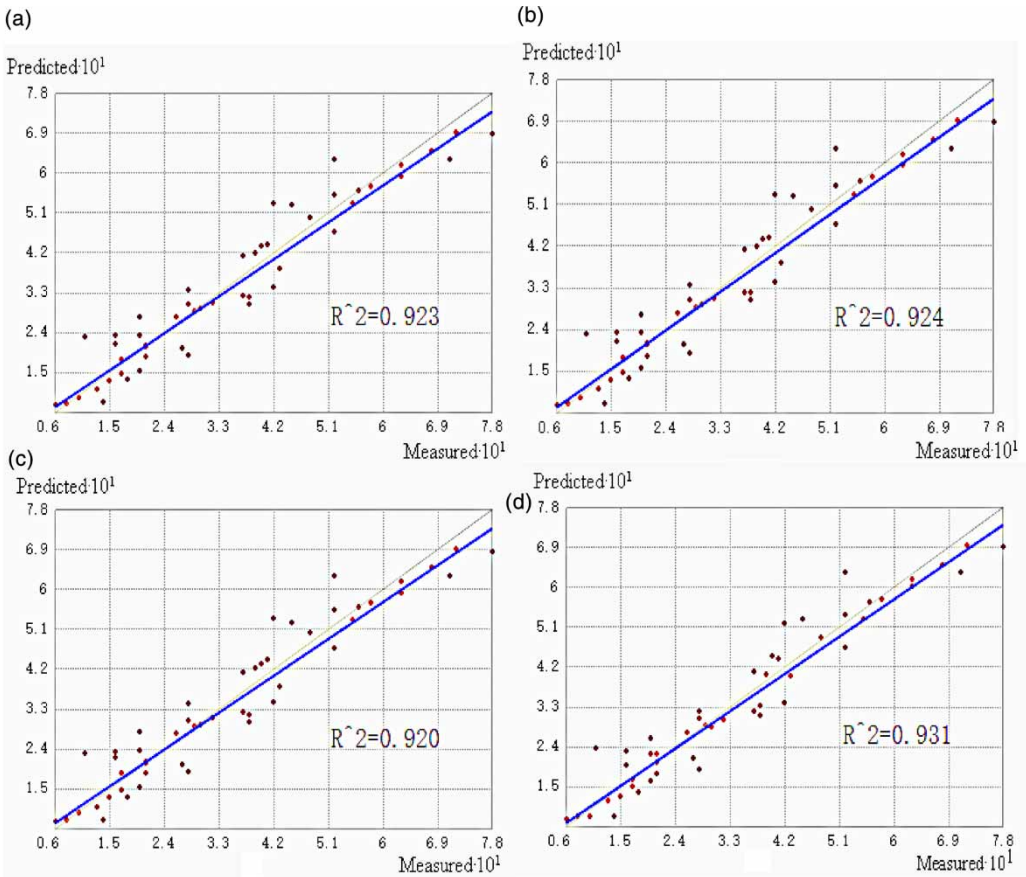

Figure 6 | Cross-test charts of fluoride: (a) circle model; (b) spherical model; (c) Gaussian model; and (d) exponential model.

model was used to spatially interpolate the shallow groundwater fluoride in the studied area, and the prediction was closest to the actual situation.

Anisotropy analysis

Anisotropy refers to the difference in the nature of things due to different directions (Thomsen & Anderson 2015). Therefore, anisotropy should be considered when performing spatial interpolation. Figure 7 shows that the variation of fluoride in shallow groundwater in the studied area in the northwest and southeast directions was slightly higher than in other directions, but overall did not show a significant difference, and anisotropy was not added.

Spatial distribution of fluoride

Combined with this study, the prediction results of fluoride concentration were divided into ten intervals at equal intervals. From high to low, red, cinnabar, vermilion, hemerocallis yellow, bright yellow, ochre, lotus green, bamboo moon, hair moon and sand blue, a total of ten colors were displayed. The results of spatial distribution and environmental superposition of shallow groundwater fluoride in the studied area are shown in Figure 8.

Figure 8 shows that the highest area of groundwater fluoride concentration was located in the southeast, which decreased uniformly from southeast to northwest, and the side of industrial production formed a fluoride concentration subcenter. The groundwater ridge divides the groundwater in the studied area into two areas, northwest and southeast. The weathering of the acidic bedrock in the southeast and the lithological partial clay in the groundwater caprock, and the ion exchange of groundwater and minerals are the reasons for fluoride accumulation. Hallett *et al.* (2014) studied groundwater fluoride in India and found that the excessively high local groundwater fluoride concentration was the result of weathering of the bedrock and the development of weathering layers. Salifu *et al.* (2012) used piper graph classification, correlation analysis, principal component analysis, and other methods to study groundwater fluoride in northern Ghana. It was found that the main reasons for the local groundwater fluoride exceeding the standard were the dissolution of minerals and the ion

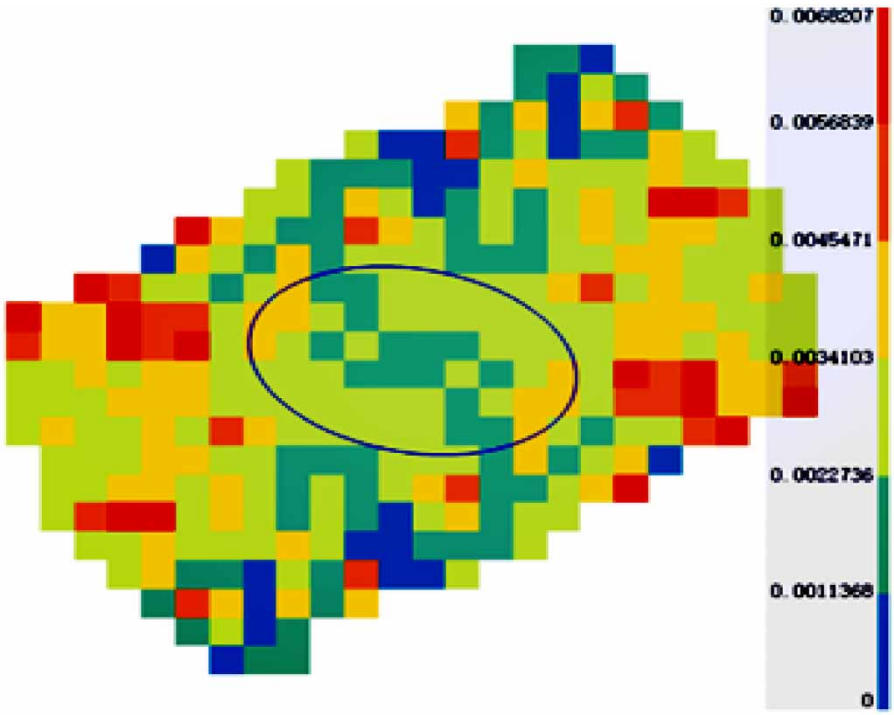

Figure 7 | Fluoride anisotropy test.

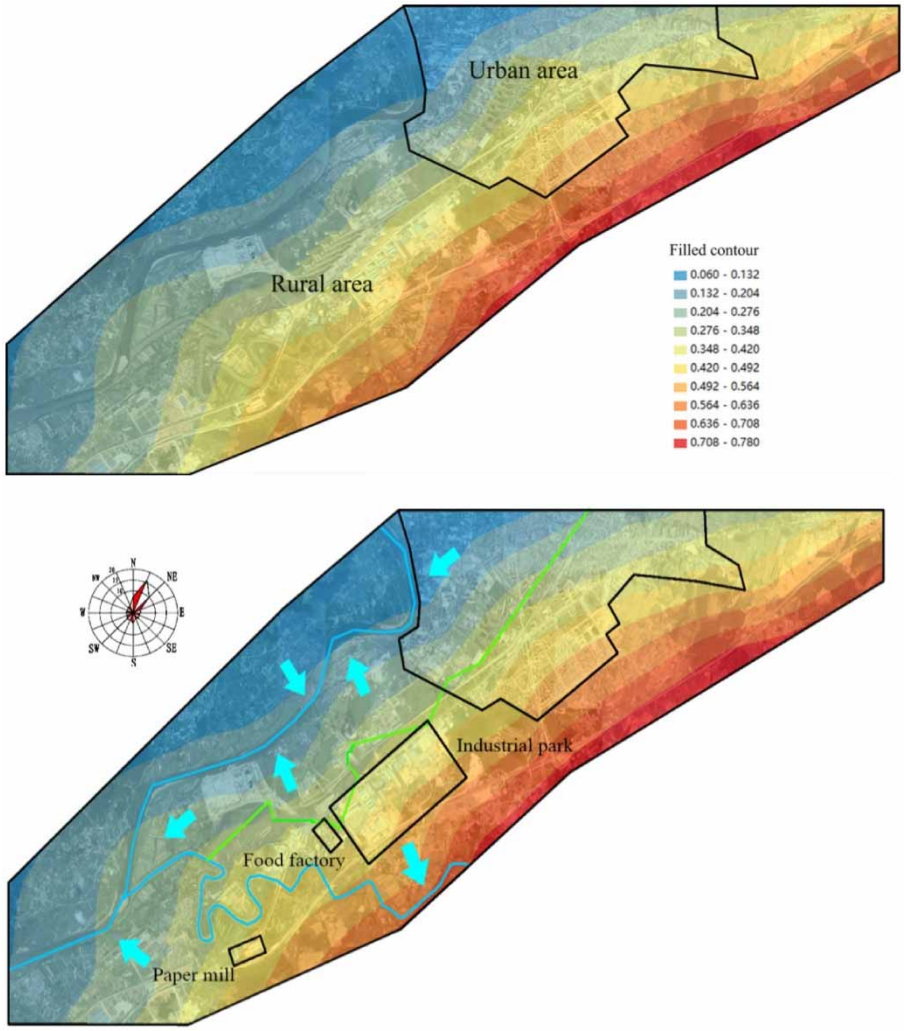

Figure 8 | Prediction map of noncarcinogenic risk spatial distribution of fluoride and environmental overlay map.

exchange between groundwater and minerals. The interval of decreasing groundwater fluoride in the studied area was more uniform, and the enrichment area was more concentrated. It was more like the result of free diffusion from line sources. If the groundwater fluoride in the studied area only came from the dissolution of bedrock, it should be shown that both the northwest and southeast are high-value areas, decreasing toward the middle.

It can be seen that fluoride was not only generated by natural factors, but coal combustion also caused fluoride pollution in groundwater. Li & Zhang (2012) analyzed the changes in groundwater fluoride in Zhangjiakou City from 2008 to 2010. The results showed that the main sources of local groundwater fluoride were geological factors and industrial coal combustion. The wind direction in the studied area was dominated by northeasterly and northerly winds, so the coal-fired flue gas adheres to the soil, and the area of pollution caused by infiltration into groundwater should be located in the southwest of the pollution source. However, no matter whether in the urban area or the agricultural area, there was no trend of increasing fluoride in the downwind area of the local dominant wind direction. There was a side of industrial production where fluoride was enriched under the joint action of factory wastewater discharge and natural dissolution of rocks, forming a subcenter of groundwater fluoride pollution. The concentration of fluoride in the northwest was low, and care should be taken to prevent the health risks of low

concentrations of fluoride. In summary, there was pollution from groundwater fluoride in the industrial park.

CONCLUSION

This study investigated the human health risk assessment and spatial distribution of fluoride in shallow groundwater in a region of southwest China. Although the fluoride concentration in the studied area did not exceed the acceptable limit (1.00 mg/L), the over standard rate of fluoride based on the background value was 34%, and the tendency of pollution was more obvious. The human health risk assessment model was used to evaluate the noncarcinogenic risk to local children and adults exposed to groundwater fluoride through multiple channels. The results showed that in the studied area, the HI values of children and adults were less than 1, and the risks were at acceptable levels. Children were more likely to be harmed by fluoride than adults. We should mainly prevent the harm of fluoride accumulation to children. Further research had shown that exposure to fluoride in groundwater through the ingestion route posed a greater noncarcinogenic risk in the area than through skin contact. Besides, HI values were less than 1 in both urban and rural areas. The spatial distribution of fluoride concentration in the region was obtained by the Kriging interpolation, and the results showed that the population in the southeast of the study area had the highest exposure to fluoride. Therefore, the fluoride in the area should be controlled to prevent the fluoride from exceeding the standard.

Human health risk assessment is a quantitative expression of the risk of carcinogenic and noncarcinogenic substances to human exposure, which can further reflect human health risks in different populations and different exposure routes. Besides, the Kriging method clarifies the spatial distribution of fluoride health risks and can intuitively and accurately predict the health risks of groundwater fluoride to human health. Future research should focus on the prediction model test, multichannel evaluation of the health hazards caused by fluoride to the human body (such as tea drinking, air contact, etc.), quantitative research on the diffusion capacity of fluoride in groundwater and the source of pollution emissions. This evaluation aims to arouse people's attention to fluoride pollution in shallow groundwater and provide a scientific basis for the treatment of fluoride.

ACKNOWLEDGMENTS

This work was co-supported by the Yue Qi Young Scholar Project, China University of Mining & Technology, Beijing, and National Key Research and Development Program of China (2018 YFC 0406404) and the Fundamental Research Funds for the Central Universities (2018 QH 03) and Research on Ecological Restoration and Protection of Coal Base in Arid Eco-fragile Region (GJNY2030XDXM-19-03.2).

DATA AVAILABILITY STATEMENT

All relevant data are included in the paper or its Supplementary Information.

REFERENCES

Abbasnia, A., Yousefi, N., Mahvi, A. H., Nabizadeh, R., Radfard, M., Yousefi, M. & Alimohammadi, M. 2019 Evaluation of groundwater quality using water quality index and its suitability for assessing water for drinking and irrigation purposes: case study of Sistan and Baluchistan province (Iran). *Human Ecolog. Risk Assess.* **25** (4), 988–1005.

Adimalla, N. & Venkatayogi, S. 2017 Mechanism of fluoride enrichment in groundwater of hard rock aquifers in Medak, Telangana State, South India. *Environ. Earth Sci.* **76** (1), 1–10.

Aghapour, S., Bina, B., Tarrahi, M. J., Amiri, F. & Ebrahimi, A. 2018 Distribution and health risk assessment of natural fluoride of drinking groundwater resources of Isfahan, Iran, using GIS. *Environ. Monit. Assess.* **190** (3), 137.

Ahada, C. P. S. & Suthar, S. 2019 Assessment of human health risk associated with high groundwater fluoride intake in southern districts of Punjab, India. *Expo. Heal.* **11** (4), 267–275.

APHA 2005 *Standard Methods for the Examination of Water and Wastewater*, 21th edn. American Public Health Association, APHA, AWWA, WPCF, Washington, DC, USA.

Biglari, H., Chavoshani, A., Javan, N. & Mahvi, A. H. 2016 Geochemical study of groundwater conditions with special emphasis on fluoride concentration, Iran. *Desalin. Water. Treat.: Sci. Eng.* **57** (47), 22392–22399.

Cai, F., Pu, L., Zhang, J., Zhao, Y. & Zhu, M. 2012 Identification of spatial economic structure in Jiangsu Province by applying exploratory. *Econ. Geogr.* **2** (3), 24–30.

Fallahzadeh, R. A., Miri, M., Taghavi, M., Gholizadeh, A., Anbarani, R., Hosseini-Bandegharaei, A., Ferrante, M. & Conti, G. O. 2018 Spatial variation and probabilistic risk assessment of exposure to fluoride in drinking water. *Food. Chem. Toxicol.* **113**, 314–321.

Fan, F., Du, D., Li, H. & You, X. 2013 Spatial-temporal characteristics of scientific and technological resources allocation efficiency in prefecture-level cities of China. *Acta. Geogr. Sin.* **68** (10), 1331–1343.

Felsenfeld, A. J. & Roberts, M. A. 1991 A report of fluorosis in the United States secondary to drinking well water. *J. Am. Med. Assoc.* **265** (4), 486–488.

Ganyaglo, S. Y., Gibrilla, A., Teye, E. M., Owusu-Ansah, E. D. G. J., Tettey, S., Diabene, P. Y. & Asimah, S. 2019 Groundwater fluoride contamination and probabilistic health risk assessment in fluoride endemic areas of the Upper East Region, Ghana. *Chemosphere* **233**, 862–872.

Hallett, B., Burgess, W. & Valsamijones, E. 2014 Mineralogical sources of groundwater fluoride in Archaen bedrock/regolith aquifers: mass balances from the Peninsular Granite Complex, southern India. In: *Egu General Assembly Conference. EGU General Assembly Conference Abstracts*, 27 April–2 May, Vienna, Austria, p.13424.

Hanse, A., Chabukdhara, M., Baruah, S. G., Boruah, H. & Gupta, S. K. 2019 Fluoride contamination in groundwater and associated health risks in Karbi Anglong District, Assam, Northeast India. *Environ. Monit. Assess.* **191** (12), 782–799.

Huang, Y., Chang, W. & He, Z. 2010 Health risk assessment of rural groundwater in Wuhan, Hubei. *J. Environ. Heal.* **27** (10), 892–894.

IRIS (Integrated Risk Information System) 2016 *Fluorine (Soluble Fluoride)*. Available from: https://cfpub.epa.gov/ncea/iris2/chemicalLanding.cfm?substance_nmbr=53 (accessed 6 March 2019).

Karami, A., Karimyan, K., Davoodi, R., Karimaei, M., Sharafie, K., Rahimi, S., Khosravi, T., Miri, M., Sharafi, H. & Azari, A. 2017 Application of response surface methodology for statistical analysis, modeling, and optimization of malachite green removal from aqueous solutions by manganese-modified pumice adsorbent. *Desalin. Water. Treat.* **89**, 150–161.

Kumar, D., Singh, A., Jha, R. K., Sahoo, S. K. & Jha, V. 2019 A variance decomposition approach for risk assessment of groundwater quality. *Expo. Heal.* **11** (2), 139–151.

Li, H. & Zhang, X. 2012 Analysis of groundwater fluoride content in zhangjiakou mountain area. *J. Hebei Inst. Arch. Civ. Eng.* **30** (3), 31–33.

Li, P., Wu, J. & Qian, H. 2012 Groundwater quality assessment based on rough sets attribute reduction and TOPSIS method in a semi-arid area, China. *Environ. Monit. Assess.* **184** (8), 4841–4854.

Li, J., Li, C. & Yin, Z. 2013 ArcGIS based kriging interpolation method and its application. *Bull. Surv. Mapp.* (9), 87–90.

Li, Y., Wang, F., Feng, J., Lv, J., Liu, Q., Nan, F., Zhang, W., Qu, W. & Xie, S. 2019 Long term spatial-temporal dynamics of fluoride in sources of drinking water and associated health risks in a semiarid region of Northern China. *Ecotoxicol. Environ. Saf.* **171**, 274–280.

Liu, J., Liu, Z. & Wang, H. 2010 Contents of arsenic, fluoride, nitrate and the health risk assessment of drinking groundwater in rural areas of Wuhan. *J. Hyg. Res.* **39** (1), 112–113.

Ministry of Environmental Protection of the PRC 2004 *Technical Specifications for Environmental Monitoring of Groundwater, HJ/T 164-2004*. China Environmental Science Press, Beijing (in Chinese).

Ministry of Environmental Protection of the PRC 2014 *Technical Guidelines for Risk Assessment of Contaminated Sites, HJ 25.3-2014*. China Environmental Science Press, Beijing (in Chinese).

Ministry of Health of the PRC 2006 *Standards for Drinking Water Quality, GB 5749-2006*. China Standard Press, Beijing (in Chinese).

Miri, M., Allahabadi, A., Ghafari, H. R., Fathabadi, Z. A., Raisi, Z., Rezai, M. & Aval, M. Y. 2016 Ecological risk assessment of heavy metal (HM) pollution in the ambient air using a new bio-indicator. *Environ. Sci. Pollut. Res.* **23** (14), 14210–14220.

Mukherjee, I., Singh, U. K. & Patra, P. K. 2019 Exploring a multi-exposure-pathway approach to assess human health risk associated with groundwater fluoride exposure in the semi-arid region of east India. *Chemosphere* **233**, 164–173.

Narsimha, A. & Sudarshan, V. 2017 Contamination of fluoride in groundwater and its effect on human health: a case study in hard rock aquifers of Siddipet, Telangana State, India. *Appl. Water Sci.* **7** (5), 2501–2512.

Ozsvath, D. L. 2009 Fluoride and environmental health: a review. *Rev. Environ. Sci. Biotechnol.* **8** (1), 59–79.

Patterson, J., Hakkinen, P. J. B. & Wullenweber, A. E. 2002 Human health risk assessment: selected Internet and World Wide Web resources. *Toxico.L* **173** (1–2), 123–143.

Salifu, A., Petrusevski, B., Ghebremichael, K., Buamah, R. & Amy, G. 2012 Multivariate statistical analysis for fluoride occurrence in groundwater in the Northern region of Ghana. *J. Contam. Hydrol.* **140**, 34–44.

Shi, Z., Yan, H., Bi, C. & Deng, L. 2017 Surface water quality monitoring in town based on Geotatistics- Kriging interpolation. *Chinese. J. Environ. Eng.* **11** (4), 2607–2613.

Staff, E. 2001 Supplemental Guidance for Developing Soil Screening Levels for Superfund Sites, Peer Review Draft. US Environmental Protection Agency Office of Solid Waste and Emergency Response, OSWER, Washington, DC, pp.9355.4-9355.24.

Thomsen, L. & Anderson, D. L. 2015 Weak elastic anisotropy in global seismology. *Agu. Fall. Meeting* **514**, 39–50.

USEPA 1989 *Risk Assessment Guidance for Superfund Volume I: Human Health Evaluation Manual (Part A)*. U.S. Environmental Protection Agency, Washington, DC.

Vyeltishchyev, Y. 1995 Ecopathology in childhood. *Paediatrics* **4**, 26–33.

Wang, Y., Xie, J. & Guo, X. 2008 Application of geostatistical interpolation method in ArcGIS. *Soft. Guide* **7** (12), 36–38.

Wang, J., Liu, Z., Gu, X. & Gaom, Z. 2009 Health risk assessment of environmental carcinogens. *Int. Med. Sci.: Hyg.* **36** (1), 50–58.

WHO 2004 *Fluoride in the Drinking-Water. Background Document for Development of WHO Guidelines for Drinking-Water Quality*. World Health Organization, Geneva, Switzerland.

WHO 2011 Guidelines for drinking-water quality. *WHO Chron* **38**, 104–108.

Wu, J. & Sun, Z. 2016 Evaluation of shallow groundwater contamination and associated human health risk in an alluvial plain impacted by agricultural and industrial activities, mid-west China. *Expo. Health* **8** (3), 311–329.

Wu, J., Li, P. & Qian, H. 2012 Study on the hydrogeochemistry and non-carcinogenic health risk induced by fluoride in Pengyang County, China. *Int. J. Environ. Sci.* **2** (3), 1127–1134.

Xu, B. & Zhang, Y. 2018 GIS-based human health risk assessment of groundwater contamination in the Jinghuiqu irrigation district of China. *J. AgroEnviron. Sci.* **37** (5), 992–1000.

Zhang, X. 2010 The duality of fluorine in the human body. *J. Chem. Educ.* **31** (2), 6–9.

Zhang, L., Huang, D., Yang, J., Wei, X., Qin, J., Ou, S., Zhang, Z. & Zou, Y. 2017 Probabilistic risk assessment of Chinese residents' exposure to fluoride in improved drinking water in endemic fluorosis areas. *Environ. Pollut.* **222**, 118–125.

Zhang, Y., Guo, C., Sun, P., Zhu, Y. & Yu, S. 2019 Groundwater health risk assessment based on spatial analysis in the Qiaomaidi watershed. *China Environ. Sci.* **39** (11), 4762–4768.

Zhong, X., Zhou, S., Huang, M. & Zhao, Q. 2009 Chemical form distribution characteristic of soil heavy metals and its influencing factors. *Ecol. Environ. Sci.* **18** (4), 1266–1273.

First received 30 June 2020; accepted in revised form 17 August 2020. Available online 5 October 2020